TOPICAL REVIEW

Progress in piezotronic and piezo-phototronic effect of 2D materials

To cite this article: Yiyao Peng *et al* 2018 *2D Mater.* **5** 042003

2D Materials

RECEIVED
30 April 2018

REVISED
26 June 2018

ACCEPTED FOR PUBLICATION
16 August 2018

PUBLISHED
7 September 2018

TOPICAL REVIEW

Progress in piezotronic and piezo-phototronic effect of 2D materials

Yiyao Peng[1,2], Miaoling Que[1,2], Juan Tao[1,2], Xiandi Wang[1,2], Junfeng Lu[1,2], Guofeng Hu[1,2], Bensong Wan[1,2], Qian Xu[1,2] and Caofeng Pan[1,2]

[1] CAS Center for Excellence in Nanoscience, Beijing Institute of Nanoenergy and Nanosystems, Chinese Academy of Sciences, Beijing 100083, People's Republic of China

[2] School of Nanoscience and Technology, University of Chinese Academy of Sciences, Beijing 100049, People's Republic of China

E-mail: cfpan@binn.cas.cn

Keywords: two-dimensional materials, piezoelectricity, piezotronic effect, piezo-phototronic effect

Abstract

Two-dimensional (2D) materials, possessing numerous remarkable properties including high electrical conductivity, optical transparency and mechanical strength, have supplied a fertile soil for theoretical research and practical application in electronics and optoelectronics. Due to a persistent need of strain sensors, microelectromechnical system (MEMS), nanorobots and active flexible electronics, piezotronic and piezo-phototronic effect of 2D materials have been attracting growing attentions in latest years. Therefore, a comprehensive and intensive understanding of piezotronic and piezo-phototronic effect of 2D materials is required. Here we review the recent progress in theoretical analysis and experimental observation of piezotronic and piezo-phototronic effect of 2D materials enabled by non-centrosymmetric crystal structure. After introducing the fundamental physics of piezotronic and piezo-phototronic effect concisely, the origination and analysis of the piezoelectricity in 2D materials are discussed in detail. Furthermore, we focus on the application in piezotronic and piezo-phototronic effect of transition-metal dichalcogenides (TMDCs) including transistor, nanogenerator, humidity sensor and photodetector. Moreover, some other 2D piezoelectric materials (PEMs) are also been summarized owing to their potential applications in piezotronics and piezo-phtotronics. Finally, some perspectives are put forward on the following opportunities and challenges for future research in this emerging field.

1. Introduction

2D materials, which bring about a series of unique properties in electrics, optics, and mechanics in contrast to their bulk crystals, are a category of ultrathin sheet-like crystals with the thickness of atomic or molecular level and a lateral dimension size generally at the micrometer scale [1, 2]. Since the pioneering works on graphene (a zero-overlap semimetal) in 2004 [3], 2D materials have attracted extensive attention. Subsequently, numerous significant researches on other 2D crystals including insulators (e.g. h-BN), semiconductors (e.g. WS_2), and metals (e.g. $NbSe_2$) [3–6], have emerged and progressed explosively. In recent years, 2D materials have been applied in electronics and optoelectronics on account of their remarkable advantages such as outstanding electrical conductivity, excellent optical response, high mechanical strength [7–9]. Specifically, the atomic-level thickness compels the transport of electrons, excitons and phonons to follow ballistic transportation rather than scattering or diffusion [10, 11]. The electronic behavior is critical for both fundamental study and novel electronics. The ultrathin nature gives rise to an excellent optical transparency and a fast response to external stimulation facilitating the applications in optoelectronic and other sensing devices [12]. Except for the properties in electrics and optics of 2D materials, the mechanical attributes also counts. 2D materials like graphene and monolayer MoS_2 possess a higher stress (Young's modulus) than that of stainless steel, which indicates the materials are almost defect-free and highly crystalline.

For most 2D materials possessing superior semiconductor properties, piezoelectricity can be combined to produce unusual device characteristics. The coupling between semiconductor and piezoelectricity comes into being an emerging fields of piezotronic effect. The first experiment design about piezotronic effect derived from the measurement of electrical properties in 1D ZnO nanowires (NWs) under applied strain. Subsequently, many research groups further demonstrated the presence of the piezotronic effect in other piezoelectric semiconductors including NWs, nanobelts and 2D membrane materials. However, although plenty of common 2D monolayer materials were theoretically predicted to be intrinsically piezoelectric successively such as h-BN, MoS_2, SnS, GaS and so on [5, 13–16], the experimental observation of piezotronic and piezo-phototronic effect in monolayer MoS_2 have firstly reported by Wang group until 2014 and 2015, respectively [9, 17–20]. A significant discovery was indicated that only odd-layer MoS_2 possesses piezoelectric coupling rather than in even-layer and bulk crystal due to the existence of inversion asymmetry. Recently, the piezotronic effect and piezo-phototronic effect of these 2D materials began to be widely applied in strain sensors, flexible electronics, photo detections and even nanogenerators (NGs), which tuned carrier generation, transport, recombination or separation of devices through external mechanical stimuli.

In this review, we primarily concern the theoretical and experimental application researches of piezotronics and piezo-phototronics in 2D crystals. First, we discuss the fundamental physics of piezotronic and piezo-phototronic effect and give a brief introduction of structure and origination of piezoelectricity in 2D materials. 2D materials break down spontaneously the 3D symmetry commonly perceived for bulk materials. Secondly, we highlight the theoretical simulation and experimental observation of piezotronic and piezo-phototronic effect in 2D materials mainly focusing on TMDCs. Moreover, some other 2D piezoelectric semiconductors are also introduced, which may possess potential application value in piezotronics and piezo-phototronics. It's such a perfect conjunction to apply piezotronic and piezo-phototronic effect into the study and exploration of the intrinsic piezoelectric properties of 2D materials. Finally, a conclusion and an outlook for the future development in piezotronic and piezo-phototronic effect of 2D materials were provided.

2. Piezoelectric principle in 2D materials

Piezotronic and piezo-phototronic effect draw an increasing number of attention that has already in a relatively mature stage, while the researches in 2D materials are also in a period of vigorous development. Simultaneously, the piezoelectric property of some 2D materials has been predicted theoretically, which means a new opportunity emerges to combine piezotronic and piezo-phototronic effect with 2D materials. Thus, theoretical fundamental of piezotronics and piezo-phototronics and the reason why some 2D materials possess piezoelectric properties are introduced as following.

2.1. Theoretical fundamental of piezotronic and piezo-phototronic effect

The theory of piezotronic and piezo-phototronic effect was first proposed in 2006 and 2010 by Wang group, respectively [23, 24]. The coupling between photoexcitation and semiconductor forms the well-known optoelectronics, while that between photoexcitation and piezoelectricity leads to the field of piezophotonics. Besides, a novel field of piezotronics based on the piezoelectric-semiconductor properties has been created, the fundamental of which is to utilize piezoelectric potential to tune and control the characteristics of charge carrier transport. Piezotronics has potential applications in active flexible electronics, human-computer interfacing, MEMS systems, nanorobotics and sensors [21, 25]. Further, the coupling among semiconductor, piezoelectric polarization and photoexcitation generates the field of piezo-phototronics, which underpins the construction of novel piezoelectric-photon-electronic nanodevices. The piezo-phototronics also can effectively improve the performance of optoelectronic devices such as light-emitting diodes (LEDs), solar cells and photodetectors (figure 1(a)) [26, 27]. To better understand piezotronic and piezo-phototronic effect, the metal-semiconductor (M–S) contact and p-n heterojunction as the fundamental construction of electronics and optoelectronics need to be compared and analyzed profoundly. The Schottky barrier height (SBH) can be effectively modulated by piezoelectric polarization charges located at the interfacial vicinity of the M–S contact to tune the properties of charge carrier transport. Assuming PEMs is n-type semiconductors at the M–S contact (ignoring the surface states), the energy band diagram and space charge distribution are seriously affected by the existence of the piezoelectric polarization charges at zero biased voltage. Upon tensile strain, positive polarization charges are induced at the M–S contact interface that captivate electrons, resulting in a lower SBH. Conversely, under the compressive strain, negative polarization charges repelling electrons are generated at the M–S contact interface, leading to a higher SBH (figure 1(b)) [28]. With regard to the energy band at p-n heterojunction upon strain (assuming only n-type semiconductor is piezoelectric at p-n junction), similar to the alterations for the SBH at M–S contacts, which is tuned by the corresponding piezoelectric polarization charges as well. The generation, separation, transport and recombination of carriers at the junction/interface of the optoelectronic devices are tuned and controlled by piezoelectric potential, which is called the piezo-phototronic effect(figure 1(c)) [29]. For a typical piezoelectric semiconductor like ZnO NW, positive piezoelectric polarization charges are induced in the $+c$ direction when applying tensile strain. A dip comes into being in the local band diagram near the p-n junction interface. Diametrically, the compression-strain-induced negative piezoelectric polarization charges repel electrons away from the interface, giving rise to a bump in the local band structure. This promising and prosperous field based on two important physical concepts of piezoelectric

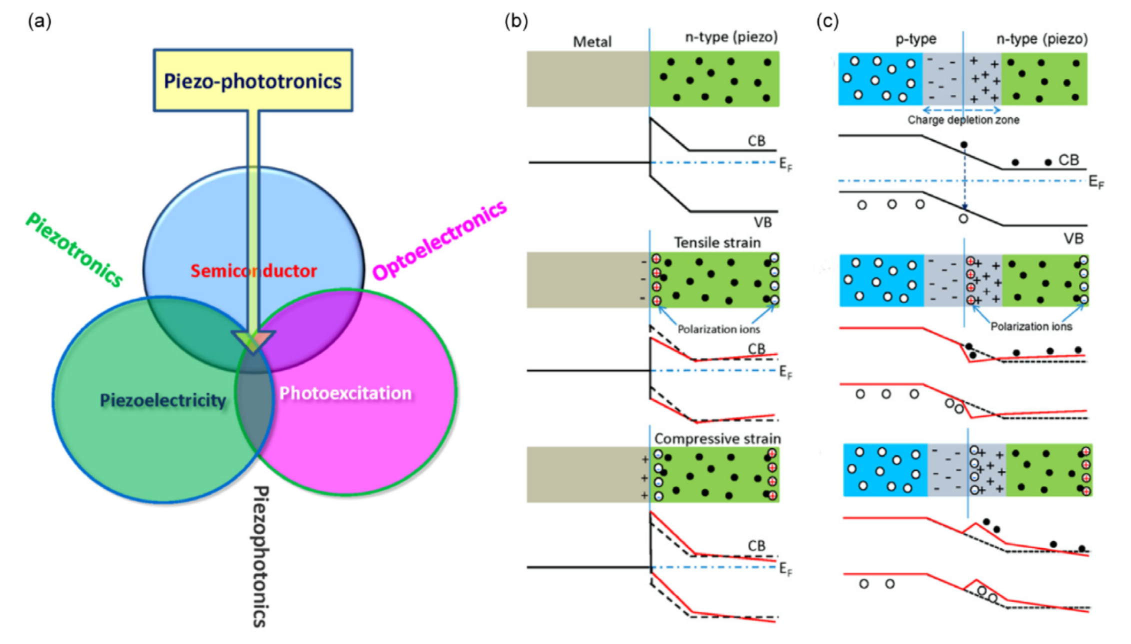

Figure 1. Fundamental theory of piezotronic and piezo-phototronic effect. (a) Schematic diagram of piezotronics, piezophotonics, optoelectronics, and piezo-phototronics on the basis of the three-way coupling among semiconductor, piezoelectricity and photoexcitation. Reprinted with permission from [21]. Copyright 2010 Elsevier Ltd. Schematic of energy band for illustrating piezoelectric effect (b) on a Schottky contacted M–S contact interface (c) on a p-n heterojunction interface (two similar band gap materials). Red lines represent the distorted band affected by piezoelectric charges. Reprinted with permission from [22]. Copyright 2012 John Wiley and Sons.

potential and semiconductor properties. Accordingly, theoretical fundamental of piezotronic and piezo-phototronic effect plays a vital role on guiding the application of novel nanodevices.

2.2. Structure and origination of piezoelectricity in 2D materials

First-principles for the piezoelectric coefficients prediction of monolayer hexagonal boron nitride (h-BN), transition metal dichalcogenides (TMDCs), group-III monochalcogenides and group IV monochalcogenides uncover that lots of these materials present a strong piezoelectric coupling [30]. Figure 2 shows the structure and origination of piezoelectricity in 2D materials. For hexagonal structures with a D_{6h} point group, such as h-BN and many TMDCs (MX_2, M = transition metal, X = chalcogenide; i.e. MoS_2, $MoSe_2$, WS_2 and WSe_2), as well as layered orthorhombic structure with a D_{4h} point group, such as group-III monochalcogenides (MX, M = Ga or In, X = S or Se), their symmetry is reduced to the D_{3h} group when thinned down to monolayer, as shown in figures 2(a)–(c) [15]. In the vertical view, similar honeycomb structure can be observed where contiguous sites are occupied by two commutative elements, while the side views of these monolayer crystals along axis x present the different structures [14]. Comparing the atomically thin h-BN, single-layer TMDC sublattice contains two chalcogenide atoms at $z = \mathrm{h}$ and $z = -\mathrm{h}$, and a transition metal is contained in the other sublattice at $z = 0$, whereas monolayer group-III monochalcogenides are four-atom thickness stacked as X–M–M–X structure with mainly covalent bonding (figures 2(e)–(g)) [16]. It can be seen that monolayer h-BN, TMDCs or group-III monochalcogenides do not have an inversion center. Another monolayer structure of 2D semiconductor materials, group IV monochalcogenides (MX, M = Sn or Ge, M = Se or S), are presented in figures 2(d) and (h) with a C_{2v} point group [15]. Their orthorhombic monolayer structures are non-centrosymmetric, which are responsible for piezoelectric phenomena. As a piezoelectric material, it needs to exhibit inversion asymmetry [31]. In terms of MoS_2, bulk MoS_2 possesses a center of symmetry between the stacked layers boned by van der Waals force [32]. Thus, bulk MoS_2 do not have piezoelectricity. However, if a single layer of MoS_2 is peeled to remove the center of symmetry, piezoelectricity will be obtained. Additionally, Wang Group and Zhang Group explored the influence of the number of MoS_2 atomic layers in strain sensors [9, 17]. Even-number-layers MoS_2 flakes do not exhibit a piezoelectric response due to the existence of inversion symmetry (figure 2(i)). On the other hand, lacking inversion symmetry, MoS_2 flakes with an odd number of layers will generate piezoelectric output and it decreases with the increase of number of layers. Upon strain, a dipole moment can be generated on account of the relative displacement between the centers of the cations and anions, which exhibits macroscopic piezoelectric potential when superposing the dipole moments created by all units in the crystal [33]. As for the unit of MoS_2, the Mo and S atoms are hexagonally coordinated, and the centers of cations and anions overlap each other in the strain free state. Under applying tensile or compressive stress, a displacement between the center of Mo^{4+}

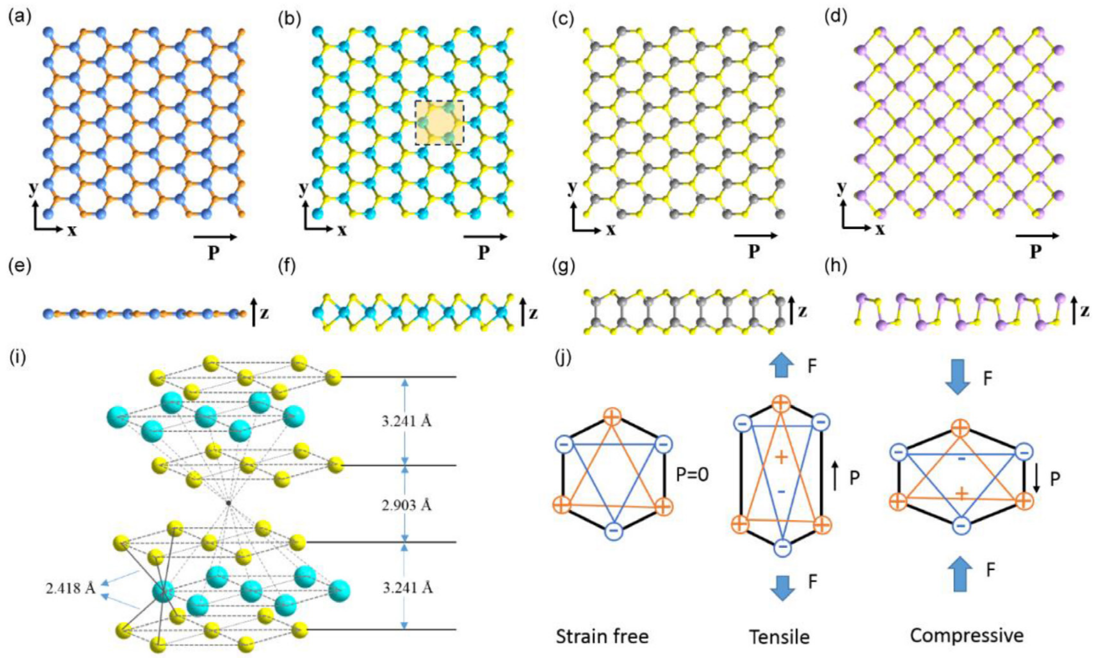

Figure 2. Structure and origination of piezoelectricity in 2D materials. Single-layer vertical view geometry of (a) h-BN, (b) MoS_2, (c) GaS and (d) SnS where nitrogen atoms are light blue, boron atoms are orange, molybdenum (transition metal) atoms are sky blue, gallium (group-III) atoms are grey, stannum (group IV) atoms are lavender and sulfur (chalcogenide) atoms are yellow. The axes and direction of piezoelectric polarization after uniaxially stretching the monolayer along the *x* direction are labeled. Lateral view of (e) the atomically thin h-BN monolayer, (f) the 2H–MoS_2 monolayer, (g) four-atom thickness stacked as X–M–M–X GaS monolayer and (h) SnS monolayer with C_{2V} structure. (i) The atomic model of two-layers MoS_2 with a centre of inversion symmetry. (j) The atomic structure model of piezoelectric potential generation in monolayer MoS_2 corresponding to the shadow area in (b).

and the center of S^{2-} proceeds, therefore piezoelectric potential will be induced (figure 1(j)). So far, a great number of theoretical calculations demonstrate many 2D materials possess piezoelectric properties and they become candidates for piezotronic and piezo-phototronic devices. Theoretical research on piezotronic and piezo-phototronic effect could provide a firm support to explore the experimental observation and practical application in piezoelectricity of 2D materials.

3. Piezotronics and piezo-phototronics and their application in 2D TMDCs

Although lots of 2D semiconductors have been predicted theoretically to possess piezoelectric properties owing to the presence of inversion asymmetry in the single-atomic structures [14, 30, 34], only some 2D TMDCs have been observed experimentally and applied in various piezotronic and piezo-phototronic devices. Indeed, 2D TMDCs are expected to be high-performance (opto)electromechanical materials for piezotronic and piezo-phototronic devices by the virtue of their remarkable semiconducting properties [32, 35], high crystallinity, outstanding mechanical properties [36, 37] and excellent optical transparency. The application based on 2D TMDCs in piezotronics and piezo-phototronics are well under way, including sensors, transistors, NGs and photodetectors. Relevant theoretical simulation and experimental study have also been discussed deeply since 2014.

3.1. Theoretical simulation of piezotronics and piezo-phototronics in 2D MoS_2

Theoretical simulation about application is indispensable to provide a compressive guidance for practical devices design. MoS_2, acting as a kind of significant piezoelectric semiconductor, has many potential applications in piezotronics and piezo-phototronics such as NGs and solar cell. The dependence of MoS_2 piezoelectric NGs on static behavior, dynamic output, high-frequency mechanical signals were simulated by Wang group [38]. A typical model of a MoS_2 NG consisting of three-layer MoS_2 sandwiched by two electrodes and an external load resistor R_{Ex}, where the zigzag edge of MoS_2 contacts with the electrodes (figure 3(a)). The static electrical characteristics, including open-circuit voltage, surface piezocharge, capacitance, of odd- and even- layer MoS_2 NGs were theoretically calculated. Specifically, the odd-layer MoS_2 NGs have piezoelectric output rather than the even-layer MoS_2 NGs owing to the presence of inversion asymmetry (figure 3(b)). Moreover, the capacitance of the MoS_2 NGs is much smaller (an order of magnitude) than that of NGs based on NWs or films [40], which provides a profound opportunity in application of high-frequency stimulation MoS_2 NGs (figure 3(c)). The striving direction of improving the fabrication techniques and optimizing the NGs circuit was also pointed out. As we know, some piezoelectric semiconductors like ZnO NWs have been relatively maturely applied in multifunctional opto-

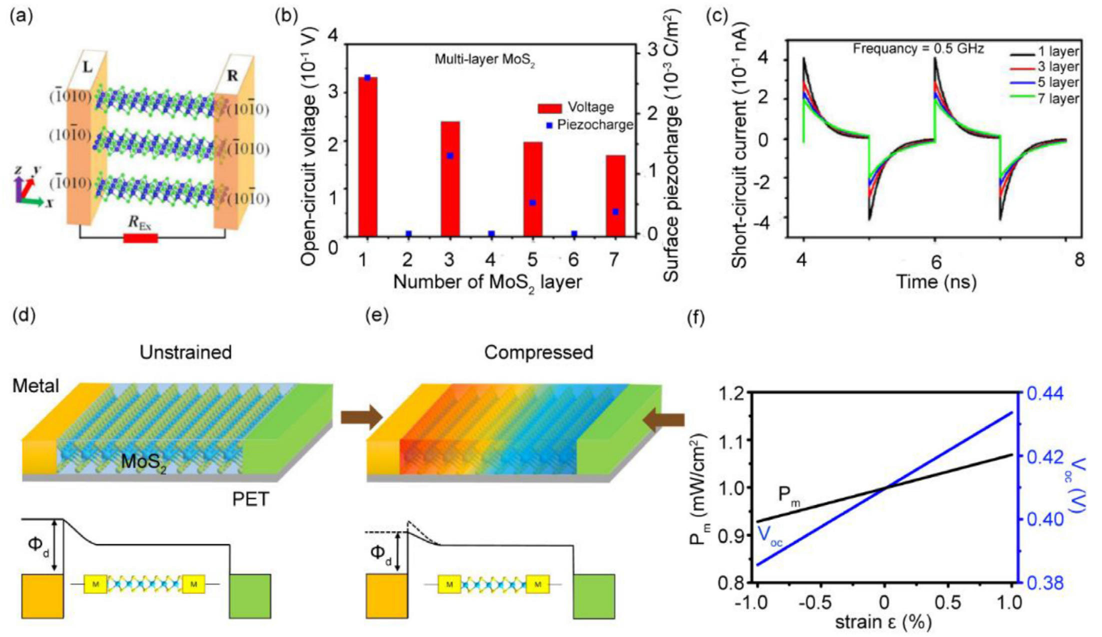

Figure 3. Simulation of 2D MoS_2 piezoelectric NGs. (a) Schematic model of a MoS_2 piezoelectric NG connected with an external load resistor R_{Ex}. (b) Effect of the number of MoS_2 layer on the NG surface piezocharge and open-circuit voltage under a 0.5% tensile strain. (c) Short-circuit currents of odd-layer MoS_2 NGs under a periodical applied strain with a frequency of 0.5 GHz. Reprinted with permission from [38]. Copyright 2016 Springer Nature. Schematic and corresponding energy band diagram of a monolayer MoS_2 solar cell under (d) strain free (e) tensile strain. The color code stands for the distribution of piezoelectric potential at the 2D monolayer MoS_2. (f) Maximum output power and open circuit voltage under different applied strain. Reprinted with permission from [39]. Copyright 2017 Elsevier Ltd.

electro-mechanical devices such as photocell, photodetector, LED [41–43]. However, the corresponding study based on 2D materials is relatively rare. Hence, theoretical researches with guiding significance is extremely important. A piezo-phototronic solar cell based on single-layer MoS_2 M–S contact was studied theoretically by Zheng *et al* [39]. The theoretical model and energy band diagram of piezo-phototronic solar cells consisting of an intermediate monolayer MoS_2, the M–S contact (left side) and Ohmic contact (right side) are presented in figure 3(d). Piezoelectric field induced by tensile strain can decrease the Schottky barrier at the contact surface and enhance built-in potential, as well as assist to separate electron–hole pairs in M–S contact (figure 3(e)) [28]. The variation of maximum output power P_m and open circuit voltage V_{oc} as a function of applied strain were shown in figure 3(f). The piezo-phototronic effect can enhance the open-circuit voltage about 5.8% when W_{piezo} (the width of charges distribution) is 0.25 nm with applied strain of 1%. Moreover, if the strain of 2D material could be increased to 11%, the ratio γ (describing the modulation for open circuit voltage of piezo-phototronic solar cell by piezoelectric charges) would reach even up to 10 times on the above situation. Thus, the mechanism based on piezo-phototronic effect may actually provide a novel way to develop high output performance 2D solar cells. These theoretical results provide not only the physical fundament for understanding the piezotronic and piezo-phototronic effect in 2D materials like MoS_2, $MoSe_2$ and WSe_2, but also the guidance for designing 2D piezoelectric nanodevices.

3.2. Piezotronics on 2D MoS_2-based transistors

Theoretical calculation has predicted many 2D crystals possess piezoelectricity due to the structurally inversion asymmetric. To quantify the experimentally piezoelectric response and measure piezoelectric coefficient (e_{11}) of 2D crystal, Zhang group reported piezoelectric response in a free-standing monolayer MoS_2 with a measured piezoelectric coefficient of $e_{11} = 2.9 \times 10^{-10}$ C m^{-1} through an approach that combines nano-indentation in an atomic force microscope (AFM) and a laterally applied electric field [17, 44, 45]. Each unit cell comprises two S atoms occupying the same site and one Mo atom residing in the opposite site in the hexagonal lattice, which destroys inversion symmetry in the *x*-*y* plane [36]. When an external electric field along armchair direction is applied, the internal piezoelectric coupling is generated by stretching the Mo-S bond (figure 4(a)). Figure 4(b) shows the device to measure the in-plane piezoelectricity, in which monolayer MoS_2 was suspended on two hydrogen silsesquioxane posts and clamped underneath by two Au electrodes. The load on the cantilever was changed by the induced stress corresponding to the deflection of a laser beam. The piezoelectric coefficient of monolayer MoS_2 can be calculated through nano-indentation and electromechanical actuation, which

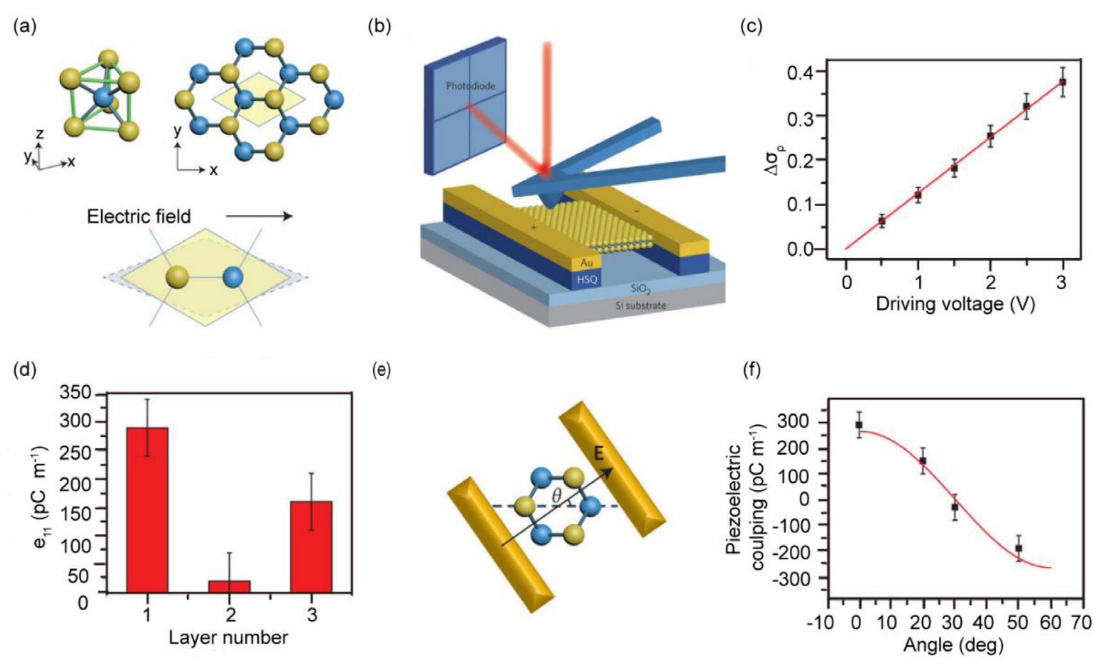

Figure 4. Ascertaining the piezoelectric coupling in free-standing single-layer MoS_2. (a) The structure and generation of piezoelectricity of MoS_2. The region denoted by the yellow shadow represents a unit cell. (b) Measurement of the in-plane piezoelectric stress. (c) The piezoelectric coefficient calculated through the linear relationship between piezoelectric stress and various driving voltage. (d) Measured piezoelectric coefficient in different number of MoS_2 membrane layers. (e) The schematic diagram of crystal's azimuthal angle θ. (f) Angular-based piezoelectric response in monolayer MoS_2. Reprinted with permission from [17]. Copyright 2014 Springer Nature.

is closed to the reported value calculated by DFT and can be comparable to some bulk PEMs such as GaN [46] (figure 4(c)). In addition, the thickness effect on the piezoelectric coefficient of mechanical exfoliated MoS_2 flakes indicates that only odd-layer membranes can exhibit a piezoelectric response due to their broken inversion symmetry, as presented in figure 4(d). Moreover, piezotronic effect is also closely related to the 2D crystal orientation. The piezoelectric coupling of these devices measured at different angles inferred from SHG fit well to a cosine curve [47] (figures 4(e) and (f)). The achievement on 2D piezoelectric device may be applied in future low-power logic switches, nanoscale electromechnical systems, ultrasensitive sensors based on a single atomic unit cell.

The potential applications of piezoelectric device based on 2D materials stimulate more interest. Subsequently, piezotronic effect in CVD-grown MoS_2 piezotronics under isotropic mechanical deformation was studied by Zhang group [48]. The fabricated device consists of a single-layer triangular MoS_2 and several sets of source/drain (S–D) electrodes (figure 5(a)). A contact-mode AFM plays the role of a gate in the whole measurement setup for the device (figure 5(b)). The load-dependent deformation applied by AFM tip of the single-layer MoS_2 piezotronics was illustrated in figure 5(c). To investigate transport behaviors of the devices, the relationship of loading location to tensile/compressive strain was uncovered (figure 5(d)). The strain-induced polarization charges alter the SBH on both contacts, as a consequence of producing a change in conductivity of the MoS_2 devices (figure 5(e)). Moreover, a high gauge factor of 1160 was found. Simultaneously, as a strain sensor, the dependence of current response on time was measured under a periodically switched applied load (figure 5(f)). Since the experimental researches on silicon-based MoS_2 transistors, piezotronic effect in 2D materials are expected to apply in CMOS technology, touch sensors.

3.3. Piezotronics on 2D TMDCs-based NGs

As mentioned above, monolayer MoS_2 has been predicted to be strongly piezoelectric [14], which can be applied in piezotronic sensor and mechanical energy harvest [49, 50]. However, until 2014, the first experimentally research of the piezotronic effect in the atomically thin 2D materials was reported by Wang and Hone groups, which made it clear that periodic releasing and stretching of thin MoS_2 membrane with an even and odd number of layers produce a zero and finite piezoelectric response, respectively [9]. The piezotronic effect was researched by applying external strain to the fabricated flexible devices where the electrons can be driven to external circuit when stretching the substrate [51], otherwise, electrons flow back in the opposite direction when releasing the substrate, as shown in figure 6(a). To avoid sample slippage, the applied strain have to be limited to 0.8% [52]. To facilitate applying strain to the device, MoS_2 membrane was transferred onto a polyethylene terephthalate (PET) flexible substrate using a wet transfer method [53]. Then the electrodes of Cr/Pd/Au were deposited to obtain M–S–M

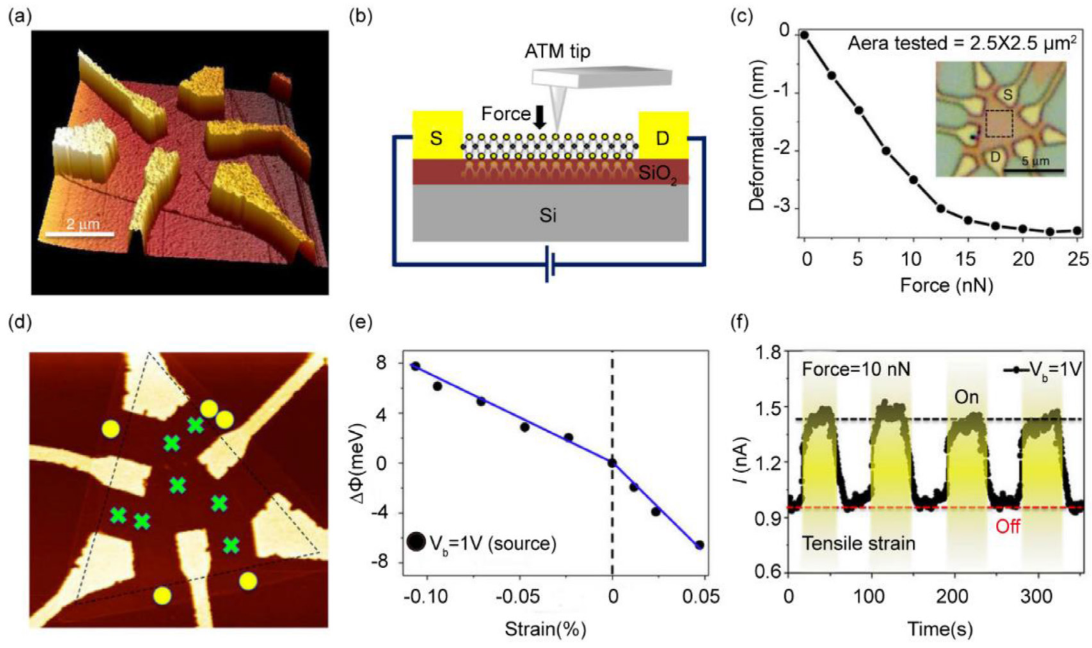

Figure 5. CVD-grown atomic-monolayer triangular MoS_2 piezotronics. (a) Illustration of a MoS_2 monolayer device with several sets electrodes. (b) Schematic illustration of the measurement device of a MoS_2 piezotronics. (c) Deformation of the MoS_2 monolayer under different applied force. (d) The relation of loading location to tensile/compressive strain, where experimental observations indicate that the MoS_2 monolayer undergoes tensile strain when force is applied near the edges (yellow circles) versus compressive strain when applied at the central zone (green crosses). (e) The derived change of the SBH as a function of strain at a bias voltage of 1 V. (f) Current response of the MoS_2 piezotronics. Reprinted with permission from [48]. Copyright 2015 Springer Nature.

junction parallel to the 'zigzag' direction (armchair: x axis; zigzag: y axis) determined by SHG (figures 6(b) and (c)). A piezoelectric output can be measured by stretching 2D MoS_2 flakes with odd number of layers rather than in even number of layers or bulk flake corresponding to the theoretical simulation mentioned above (figure 6(d)). A monolayer MoS_2 device produces a voltage of 15 mV and a current of 20 pA corresponding to maximum instantaneous power under 0.53% strain. Affected by tensile and compressive strain, the current–voltage curve shifted leftwards and rightwards, respectively. A significant characteristic of piezotronic effect is asymmetric modulation of carrier transport under opposite drain bias by strain (figure 6(e)) [21]. Theory of M–S Schottky contact in piezotronic effect can be used to explain the mechanism of the flexible 2D MoS_2 device, which further demonstrates the construction of an atomic-thin self-powered nanosystem [54] (figure 6(g)). Afterwards, directional dependent piezotronic effect in monolayer MoS_2 grown by CVD for flexible piezoelectric NGs were reported by Sang-Woo group [18]. It was discovered that the output power obtained from the NG in the armchair direction of MoS_2 is about two times higher than that in the zigzag direction of MoS_2 under the same strain of 0.48%. The researches provide a new way to effectively harvest mechanical energy using novel flexible piezoelectric NGs based on 2D semiconducting piezoelectric MoS_2 for powering low energy-consuming electronics and realizing self-powered sensors.

Considering insufficient mechanical durability for sustained operation of monolayer TMDCs materials [36, 56], bilayers WSe_2 fabricated via turbostratic stacking with reliable piezoelectric properties has been reported by Sang-Woo group recently [55]. A schematic illustration of the piezoelectric energy harvesters with two Cr/Au electrodes deposited onto the monolayer WSe_2 on a PET substrate was depicted in figure 7(a). An optical image of the electrode configuration with a 100 μm width and a 50 μm length and the inset is a photo image of the fabricate device of piezoelectric energy harvester (figure 7(b)). As for bilayer-WSe_2, five stacking structures including AA, AB, AA′, AB′, A′B are allowed [18, 47, 57, 58], where AA and AB stacking exhibit polarity in the same direction whereas AA′, AB′, and A′B show polarity in the opposite direction. Compared with AA and A′B staking structures, the other three staking structures, AB, AA′ and AB′, have relatively low energies through DFT calculations [55]. Particularly, the AA′ stacking mode possessing the centrosymmetric structure is the most stable, which is the most common (2H) form of b-WSe_2 with Bernal stacking [14]. In order to increase its piezoelectricity, a monolayer WSe_2 via CVD transferred onto another monolayer WSe_2 forming bilayer WSe_2 (tb-WSe_2) enhance degrees of freedom on symmetric bilayer 2D crystal. The schematic illustration of stacking structure and simulated piezoelecric coefficient of monolayer and five stacking modes are shown in figures 7(c) and (d). Actually, bilayer TMDCs are noted by their outstanding mechanical durability. A

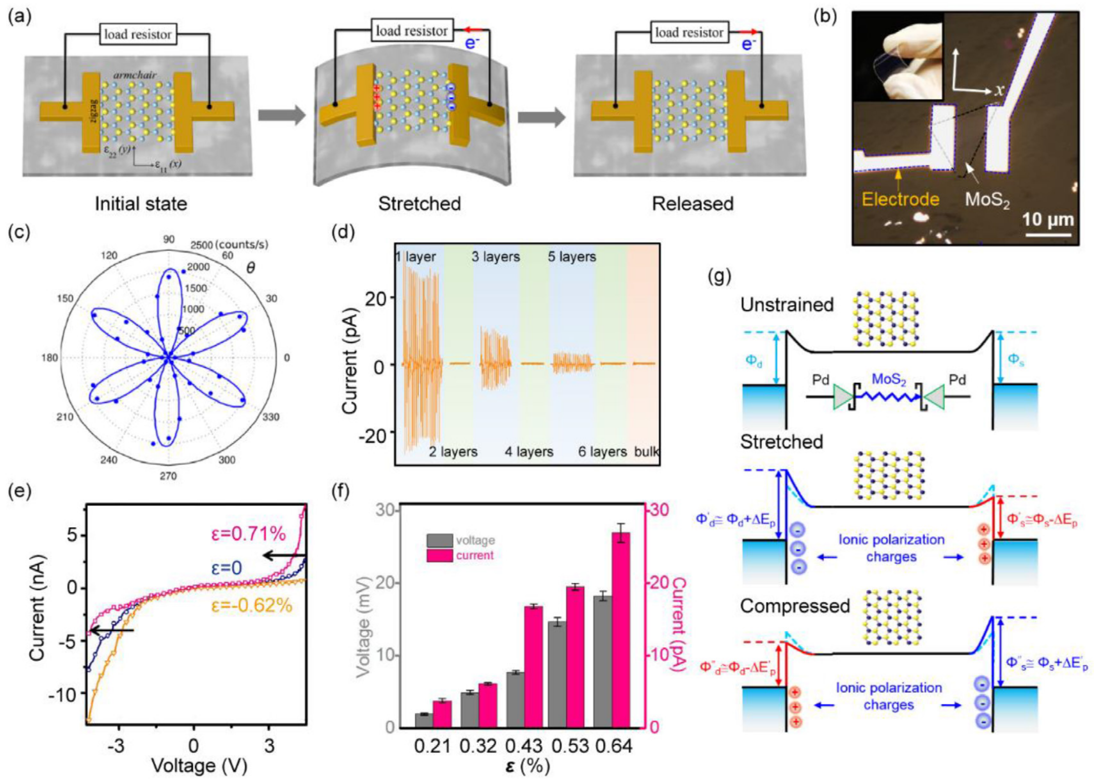

Figure 6. 2D MoS_2 for piezotronics and energy conversion. (a) Operation diagram of the single-layer MoS_2 NGs. (b) Optical photo of MoS_2 NGs and electrodes along the armchair direction. (c) Polar plot of SH intensity from single-layer MoS_2. (d) Piezoelectric outputs under different number of MoS_2 atomic layers. (e) The asymmetric modulation of carrier transport under strains in monolayer MoS_2 NGs. (f) Dependence of piezoelectric response from this monolayer MoS_2 NGs on increasing applied strain. (g) Band diagrams accounting the piezotronic behaviors observed in a single-layer NGs as a consequence of the changes in SBH by strain-induced polarization. ϕ_d and ϕ_s represent the SBH formed at drain and source contacts, respectively. ΔE_p indicates the change in SBH by piezoelectric polarization charges. Reprinted with permission from [9]. Copyright 2014 Springer Nature.

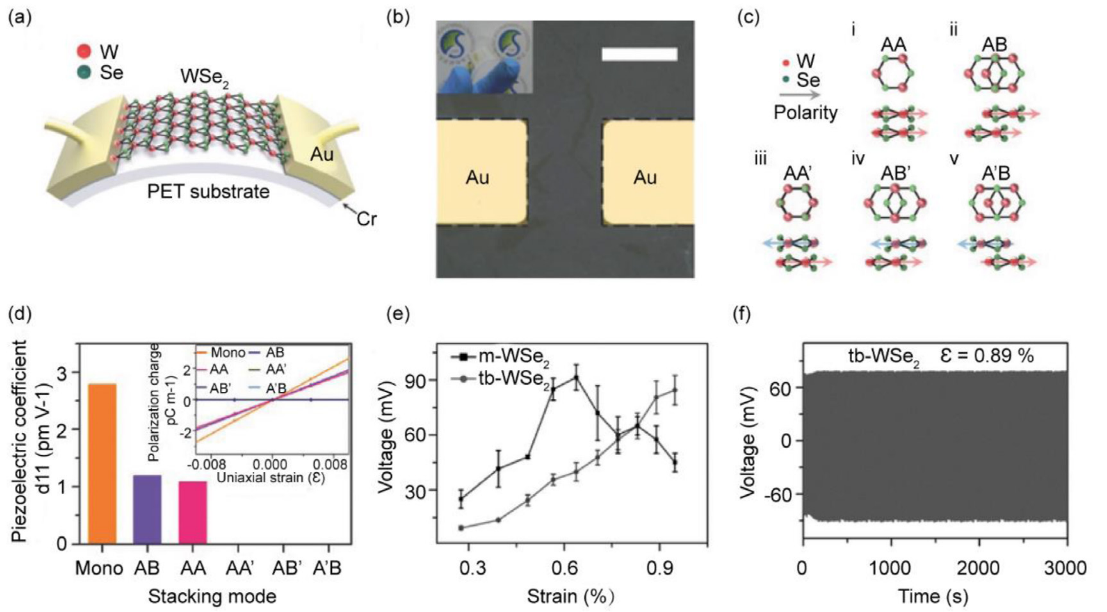

Figure 7. Reliable piezoelectricity in bilayer WSe_2 for piezoelectric NGs (a) Schematic diagram of the piezoelectric energy harvester based on monolayer WSe_2. (b) Optical image of the electrode configuration and flexible electronics. Scale bar: 50 μm. (c) Stacking structure for bilayer-WSe_2. (d) Simulated piezoelectric coefficient (d_{11}) of different stacking structure. (e) Dependence of piezoelectric peak output voltages of tb-WSe_2 and m-WSe_2 on strain with load resistance of 1 GΩ. (f) The measurement of mechanical stability of the piezoelectric energy harvesters based tb-WSe_2 with strain of 0.89% for more than 1000 cycles. Reprinted with permission from [55]. Copyright 2017 John Wiley and Sons.

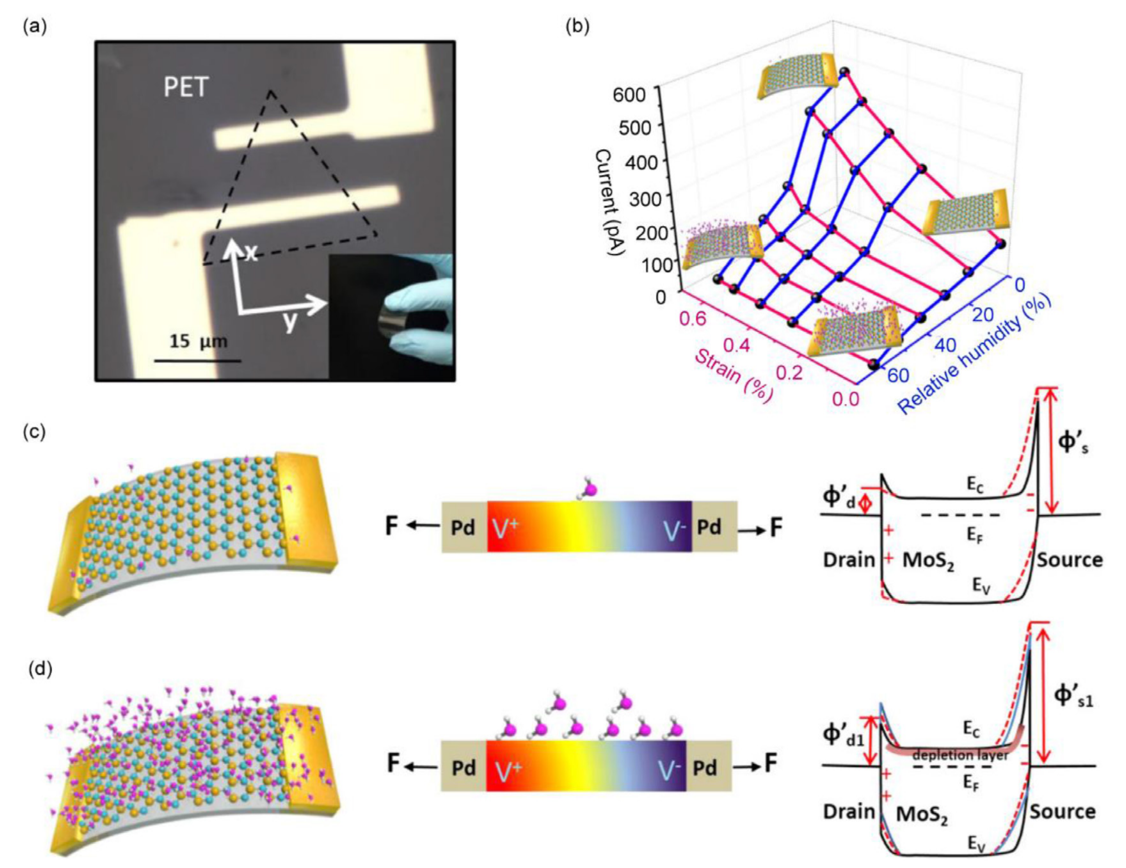

Figure 8. Monolayer MoS_2-based flexible humidity sensor enhanced by piezotronics. (a) Optical photo of flexible monolayer MoS_2 humidity sensor. (b) 3D diagram illustrating output current response under different applied strain and relative humidity at the bias of 10 V. Energy band diagram depicting a monolayer-MoS_2-based humidity sensor under (c) low relative humidity under tensile strain, (d) high relative humidity under tensile strain. Reprinted with permission from [59]. Copyright 2018 American Chemical Society.

prominent mechanical durability up to strain of 0.95% can be obtained from the bilayer WSe_2 NGs (figure 7(e)). The durability test results also reveal the tb-WSe_2 presents a better mechanical stability than monolayer WSe_2 under applied strain of 0.89% as well as reliable energy harvesting performance (figure 7(f)). In addition, all these approaches mentioned above could be employed in other 2D TMDC piezoelectric energy harvesters for various electronics.

3.4. Piezotronics on 2D MoS_2-based humidity sensor

The humidity detection has extensive application in a variety of fields such as biology, agriculture, medicine and so on. Piezotronics enhanced flexible humidity sensor can not only defeat traditional 1D materials due to their superior attractive properties, but also settle the difficulty from a high gate bias in single-layer MoS_2-based FET sensor [60, 61]. In this view, a more simple and stable way to enhance the sensitivity of humidity sensor based on 2D materials by piezotronic effect has been reported by Wang Group [59]. The device adopts a typical structure of back-to back Schottky contact on single-layer MoS_2 (figure 8(a)). For visual observation, a 3D graph consisting of the relationship among current response, applied strain and relative humidity is plotted in figure 8(b). When bending the device upward to obtain tensile strain, a larger current output and an enhanced sensitivity for the humidity sensing are achieved owing to piezotronic effect. Actually, the mechanism of humidity sensing in the MoS_2-based devices is the process of charge transfer [60]. When the surface of MoS_2 device channel absorbs environmental water molecules, the output current will change greatly. Moreover, the principle why piezotronic effect enhanced the performance of the humidity sensor is shown in figures 8(c) and (d). In the condition of low relative humidity, the capacity of water to trap electrons from monolayer MoS_2 surface is extremely weak, so the SBH at energy band are mainly dominated by the applied external filed and M–S contact. Conversely, when plenty of water molecules are absorbed on the MoS_2 surface under high relative humidity, electronic transport of the conduction band is reduced effectively owing to numerous electrons captured by water molecules. Furthermore, piezoelectric potential is introduced by applied tensile strain, which decreases the SBH for electrons at the junction. Therefore, the observed output current and humidity sensitivity are both enhanced due to more electrons getting through conduction band under tensile strain at a positive bias. However, the performance of the humidity sensor tuned by piezotronic effect in a low relative humidity case is stronger than that in a high relative humidity condition, which can be attributed to a better presentation of piezotronic effect with less water absorbed on the channel surface. This flexible humidity sensor enhanced by piezotonics might break through the detection limit of a low humidity and have potential applications in environment monitoring, gas sensing and so on.

3.5. Piezo-phototronics on 2D MoS_2-based photodetector

Emerging application in human–machine interfacing and wearable devices promote and manifest the importance of functional optoelectronics [64–66]. Recently, flexible function devices based on 2D materials for optoelectronics has attracted more attention. The experimental evidence of piezo-phototronic effect in flexible optoelectronics based on monolayer 2D MoS_2 was firstly reported by Wu *et al* in 2016 [19]. The optical image of the fabricated flexible device with mechanical exfoliation MoS_2 transferred on PET using the described methods above was shown in figure 9(a). For comparison, photoresponse without strain applied was showed. Subsequently, the changes in photodetection properties of the devices with strain were intensively characterized, in which photocurrent can be modulated effectively with illumination intensities under different strain (figure 9(b)). A maximum photoresponsivity of 2.3×10^4 A W^{-1} is demonstrated under a -0.38% compressive strain at low illumination intensity of 3.4 μW cm^{-2} by a 633 nm laser, which possesses a 26-fold enhancement over the reported previously highest photoresponsivity for single-layer MoS_2 phototransistors without strain applied. Actually, the gating effect induced by strain polarization plays an extremely significant role on photo-generated carriers density due to finite carrier concentration in monolayer MoS_2 at low optical illumination [9]. As for working mechanism of piezo-phototronic response in monolayer MoS_2 photodetectors, energy band diagrams can explain piezo-phototronic behaviors caused by the variation of SBH through strain-induced polarization (figure 9(c)) [21]. Furthermore, a flexible p-CuO/n-MoS_2 heterojunction photodetector tuned by piezo-phototronic effect was reported by Wang group in 2017 (figure 9(d)) [62]. To further characterize the p-CuO/n-MoS_2 heterojunction performance modulated by piezo-phototronic effect, the dependence of *I*–*V* curves on various illumination light powers and different applied strains were measured, respectively (figures 9(e) and (f)). Compared with strain-free case, photocurrent is enhanced 27 times under a strain of 0.65% at the illumination power of 1656.05 mW cm^{-2}. To pursue a better performance of flexible optoelectronics based on MoS_2 enhanced by piezo-phototronic effect, Wang Group reports a monolayer MoS_2 p-n homojunction photodiode more recently [63, 67–69]. In this device design, more efficient interface barrier and separation of photo-induced carriers are provided. A shielding layer of PMMA etched by EBL was coated on the side of MoS_2 and $AuCl_3$ solution was doped in the uncovered area after annealing. Then, Cr/Au electrodes were patterned on two sides of p-n junction to obtain Ohmic contact after transferring the as-fabricated MoS_2 homojunction on a flexible PET substrate. The measurement equipment of electrical properties and the optical image of fabricated device were indicated in figure 9(g). Photocurrent exhibits an enhancement trend with increasing tensile strains and it shows approximately 5-fold improvement under the strain of 0.51% compared to that in no strain state at the optical power intensity of 8.5 μW cm^{-2}. The specific relationship among photocurrent, strain and optical power can be understood clearly from figure 9(h). Moreover, the physical mechanism of piezo-phototronic effect enhanced the device photoresponse are elucidated in detail (figure 9(i)). Positive piezoelectric potential on the n-MoS_2 side lowers SBH (left side), while negative piezoelectric potential on the doped p-MoS_2 side raises SBH (right side), resulting in the widening of depletion zone and increasing of barrier height. Rapid separation, less recombination and accelerated transport improve the performance of photodiode. Accordingly, monolayer MoS_2 based on M–S contacts, p-n heterojunction and p-n homojunction have been applied in photodetectors tuned by piezo-phototronic effect, which lay the foundation of other novel optoelectronics and sensors. Piezo-phototronic effect in 2D atomically thin crystals may prompt the development of personal health monitoring, flexible ultrathin optoelectronics and wearable communication [70–72].

4. Potential prospect for other 2D PEM in piezotronics and piezo-phototronics

Except for the progress of piezotronic and piezo-phototronic effect used in numerous 2D TMDCs, some other 2D PEMs possess potential prospect in this emerging field. Specifically, graphene, as an intrinsically non-piezoelectric semimetal, may be engineered into a kind of novel 2D PEM with band gap and asymmetry [73–77]. Actually, piezoelectric property in modified graphene has been theoretically and experimentally reported. Additionally, graphitic carbon nitride (g-C_3N_4) nanosheets can be exfoliated from commercially available powder [78]. Piezoelectric coefficient of g-C_3N_4 nanosheets has been measured, which also can act as an alternative 2D PEM to fabricate piezotronics and piezo-phototronics. Nowadays, black phosphorus (BP) and perovskites, as research hot spots, have been fabricated into plenty of high-performance electronic and optoelectronic devices, whose potential prospect in piezotronics and piezo-phototronics is worthy investigating further

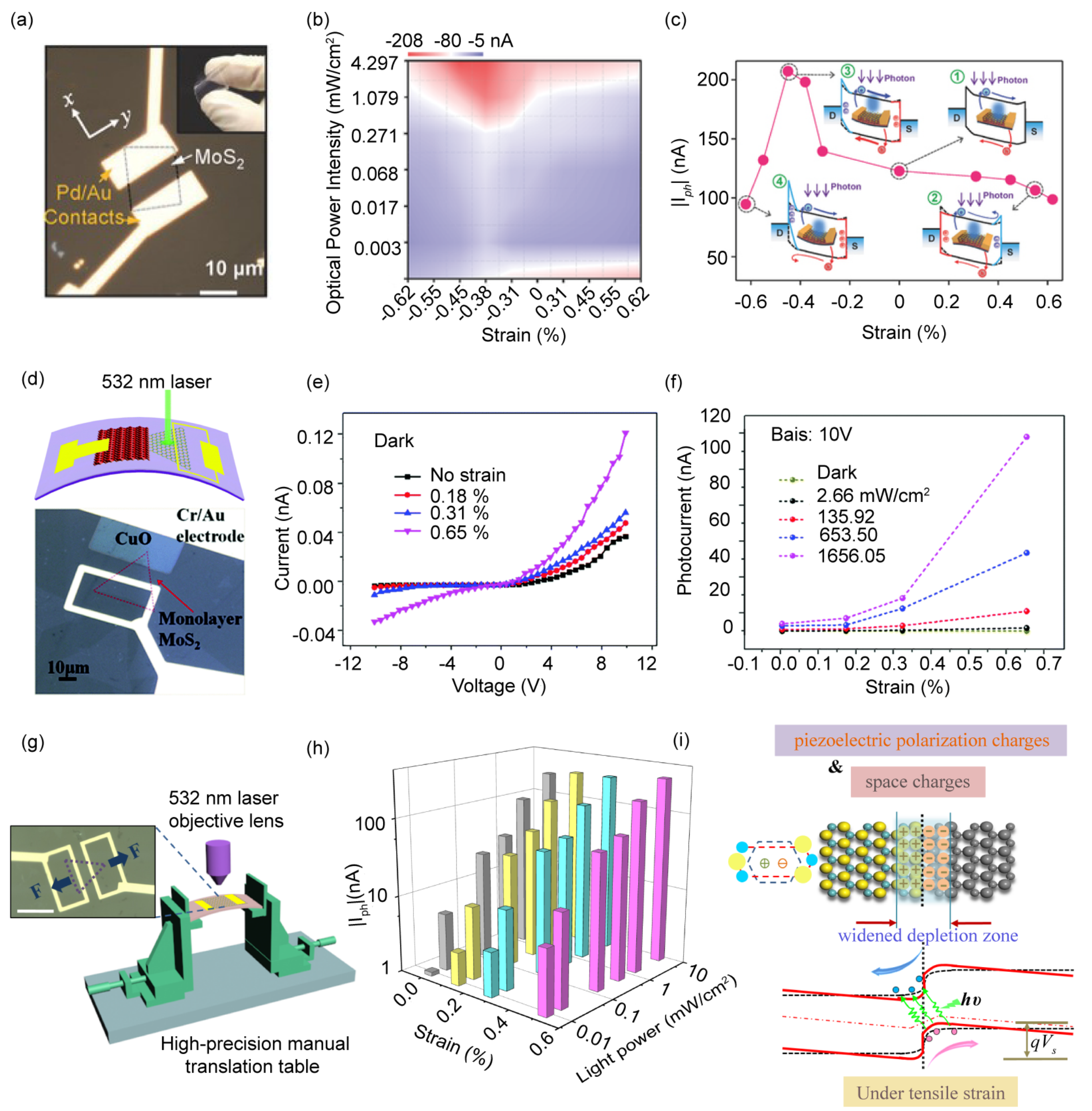

Figure 9. Piezo-phototronic effect in monolayer MoS_2 flexible optoelectronics. (a) The optical image of flexible monolayer MoS_2 piezo-phototronic device. (b) Comprehensive mapping for photocurrent in monolayer device under different mechanical strains and optical power intensities. (c) Operating mechanism of piezo-phototronic response in monolayer MoS_2 photodetector. Reprinted with permission from [19]. Copyright 2016 John Wiley and Sons. Piezo-phototronic effect in flexible photodetector based p-CuO/n-MoS_2 heterojunction. (d) Schematic illumination and optical images of the device. (e) *I*–*V* curves of the heterojunction at various tensile strains in dark. (f) The strain dependence of the photocurrent at different illumination intensities at a bias of 10 V. Reprinted with permission from [62]. Copyright 2017 Royal Society of Chemistry. Piezo-phototronic effect enhanced a monolayer MoS_2 p-n homogenous photodiode. (g) Home-made high-precision test equipment and optical device structure. (h) 3D diagram depicting photocurrent under different applied strains and various optical power intensities at the bias of −10 V. (i) Work mechanisms of strain tuned photodiode based on MoS_2 p-n homojunction under tensile strain.

[79–81]. In all, it is hopeful to combine these superior 2D PEMs into predominant piezotronic and piezo-phototronic devices in future.

4.1. Piezoelectricity in modified graphene

Graphene indeed has an inversion center and does not possess intrinsic piezoelectricity. However, after the intensive understanding for piezoelectricity, many strategies can be utilized to break the inversion symmetry of graphene theoretically, such as stacking control in graphene bilayers, holes formation, exerting nonhomogeneous strain, and chemical doping [73, 84–87]. Among these techniques, chemical doping seems to be the most prospective method since it has already represented an active experimental avenue for regulating electronic and structural properties of graphene [88]. Typically, Evan J Reed group proposed that graphene can be designed to be piezoelectric through the selective surface atomic adsorption [76]. A uniform coverage of fluorine (F), hydrogen (H), potassium (K), lithium (Li) atoms, and also two different atomic dopants on opposite sides including H and F or Li and F are considered to be doped to generate piezoelectricity in graphene, piezoelectric coefficient of which are shown in figure 10(a). Additionally, Latterly, Kh. E. El-Kelany group applied *ab initio* quantum-mechanical to dope BN inclusions into graphene according to substitutional fractions

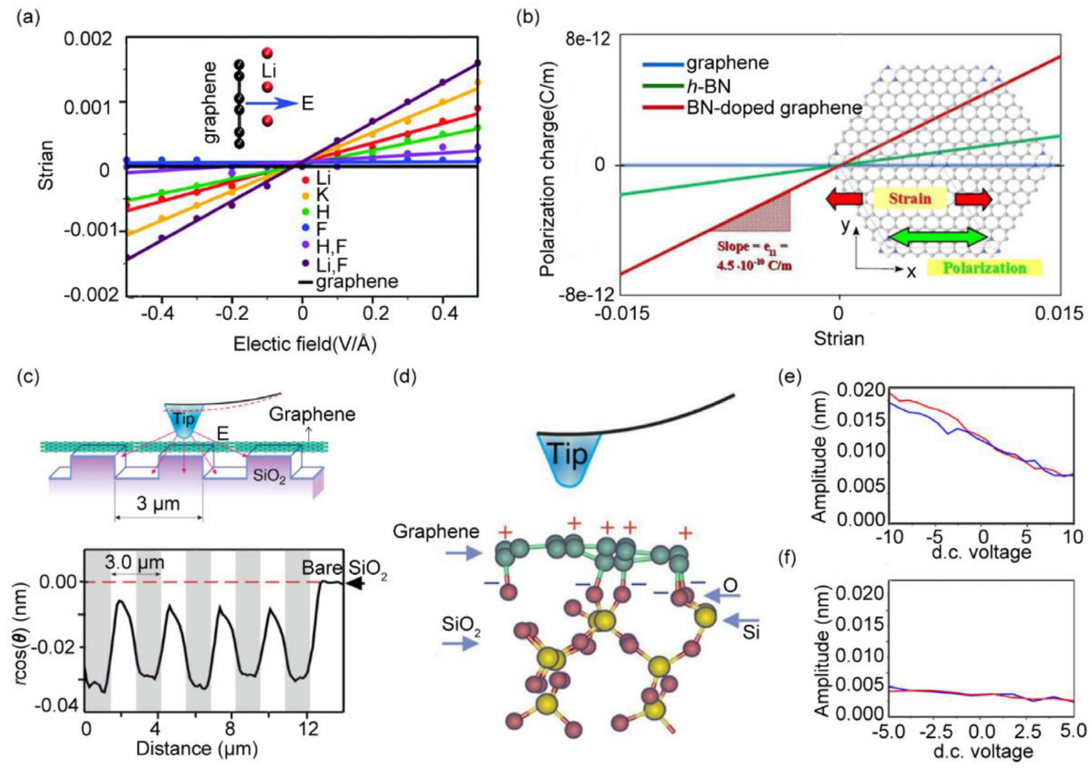

Figure 10. Properties of piezoelectricity in engineered graphene. (a) The linear relationship between strain and electric field corresponding to adsorption of various atoms, the slope represents the piezoelectric coefficient d_{31}. Reprinted with permission from [76]. Copyright 2011 American Chemical Society. (b) A finite in-plane piezoelectricity charge induced by doping different BN patterns into graphene sheets. Reprinted with permission from [82]. Copyright 2015 American Chemical Society. Experimental measurement of piezoelectric response in modified graphene. (c) Spatial variation of piezoelectric response. (d) Schematic of origin of the measured piezoelectric response. Piezoelectric voltage spectroscopy measured in a piezo-step mode on (e) supported and (f) suspended graphene, respectively, with driving a.c. voltage of 1 V and measurement frequency of 20 kHz. Reprinted with permission from [83]. Copyright 2015 Springer Nature.

and different patterns, the piezoelectricity coefficient of which has a larger magnitude than previously reported about graphene [82]. BN pairs substitute carbon pairs to achieve the noncentrosymmetric D_{3h} group instead of the centrosymmetric D_{6h} (figure 10(b)). The theoretical prediction of piezoelectricity in modified graphene is comparable to that in traditional PEMs [82]. However, the experimental observation had not be published until Andrei Kholkin group measured the piezoelectricity of chemically-modified monolayer graphene in 2015 [83]. In their experiment, the single-layer graphene synthesized by CVD was transferred onto SiO_2 calibration grating TGZ4 substrate to measure electromechanical properties via piezoresponse force microscopy (PFM) and confocal Raman spectroscopy (figure 10(c)). Compared with the suspended graphene measured barely piezoelectric response, the achieved strain and observed piezoresponse in graphene are bound up with the chemical reaction between carbon atoms of graphene and the oxygen from underlying SiO_2 [89], which induce non-zero net dipole moment and polarization charges in the research system (figure 10(d)). Consequently, enlarging/reducing the net polarization modulated by an applied electric bias to the tip leads to increasing/decreasing amplitude of the PFM signal (figures 10(e) and (f)). The results provide a basis for numerous emergent applications in which graphene/SiO_2 structures are used as a platform for actuators and sensors in future. Combining the outstanding properties of graphene, modified graphene has potential value in the application of piezotronics and piezo-phototronics.

4.2. Piezoelectricity in graphitic carbon nitride ($g\text{-}C_3N_4$)

To settle the difficulty of adding nanoscale triangular-shaped holes into graphene [90], 2D graphene nitride ($g\text{-}C_3N_4$) nanosheets was chosen as an alternative 2D structure [78]. Single-sheet $g\text{-}C_3N_4$ composed by a tri-s-triazine repetition is more energetically stable. The structure of $g\text{-}C_3N_4$ naturally possesses uniform triangular nanopores [91]. The typical size of the liquid-phase exfoliated nanosheet samples was about 800 nm in width and 1–2 nm in thicknesses (figures 11(a) and (b)). Both atomically thin and layered $g\text{-}C_3N_4$ nanosheets have been discovered to exhibit piezoelectricity. Influenced by triangular pores (non-centrosymmetric), a net average polarization could be generated in non-PEMs under uniform stress. The linear relationship between piezoelectric response and applied voltage from vertical PFM confirms the linear piezoelectricity of the nanosheet samples (figure 11(c)). Meanwhile, bulk $g\text{-}C_3N_4$ particle also possesses

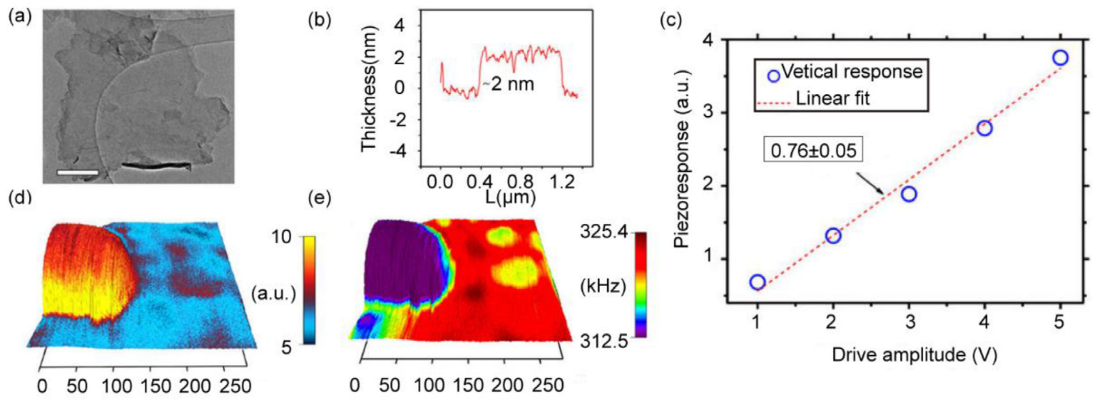

Figure 11. Properties of piezoelectricity in g-C_3N_4. (a) TEM image of exfoliated g-C_3N_4 nanosheets, scale bar, 200 nm. (b) AFM analysis of g-C_3N_4 nanosheets with an average thickness of about 2 nm. (c) Linear correlation between drive amplitude and vertical PFM responses of g-C_3N_4. (d) PFM amplitude on a g-C_3N_4 particle. (e) The mapping of resonant frequency. Reprinted with permission from [78]. Copyright 2014 Springer Nature.

a higher calculated piezoelectricity coefficient than h-BN or α-quartz (figures 11(d) and (e)). The effective vertical coefficient of the g-C_3N_4 is estimated to be approximately 1 pmV^{-1}. Higher piezoelectric response suggests that g-C_3N_4 may become a potential opportunity to assemble more sensitive (opto-) electromechanical devices.

4.3. Piezoelectricity in BP and MoS_2 van der Waals heterostructure

Past few years witness the booming development of BP owing to its superior and unique electrical and optical properties [92]. Monolayer BP is theoretically predicted to be piezoelectric from the point of inversion-asymmetry structure. The electronic band structure of monolayer BP can be modified by in-plane strains, leading to anisotropic change of carrier mobility along armchair and zigzag directions [81]. Additionally, carrier effective mass and carrier concentration of BP/MoS_2 van der Waals heterostructure was modulated by applied compressive strain, suggesting good piezoelectric effect in this heterostructure [93]. Thanks to type-II band alignment of BP/MoS_2, photo-excited electrons and holes are more likely to be separated resulting in a broad application in efficient photodetector with a great absorption coefficient in ultra-violet region. However, piezoelectricity in 2D BP has still not been demonstrated by experimental observation. We can expect the piezotronic and piezo-phototronic effect applied in BP to produce high-performance electronics and optoelectronics.

4.4. Piezoelectricity in 2D perovskites

Perovskites refer to a ternary family of crystalline materials possessing a general chemical formula ABX_3. In the past decades, oxide perovskites are relatively popular due to their prominent electrical properties including ferroelectricity, pyroelectricity, superconductivity and piezoelectricity [79]. $BaTiO_3$ is used as a piezoelectric material for the first time [94]. Organic-inorganic hybrid perovskites emerged as an excellent optoelectrical material have a great promising in the application of photovoltaic devices, which also have been synthesized into atomically thin 2D nanosheets with a thickness of about 1.6 nm and with an average length of 4.2 μm [80]. 2D perovskites may expand new horizons for the researches of 2D PEMs. However, the piezoelectric properties in 2D perovskites have barely been explored. If the piezotronics and photo-piezotronics can be combined in 2D perovskites, some revolutions may be brought in the application of solar cell and even more optoelectronics.

5. Conclusion and outlook

Despite tremendous progress in 2D materials, much works remain to be done to realize the full potential and achieve a comprehensive development such as the properties of piezoelectricity [81, 95–98]. Recent theoretical predictions of piezoelectricity in 2D materials portend that the fundamental of piezotronic and piezo-phototronic effect may offer an ideal approach for studying the atomically thin semiconductor materials [14–16, 28]. The piezotronic and piezo-phototronic effect in 2D crystals have potential application in self-power nanodevices, adaptive bioprobes, tunable and stretchable electronics and optoelectronics, which based on the strain-induced piezopotential created by polarization charges in the flakes [21]. Plenty of 2D materials like MoS_2 are centrosymmetric in their bulk but could exhibit non-centrosymmetry when thinned down to a single atomic layer. The piezoelectric coefficients of monolayer BN, MoS_2, WSe_2, GaS, SnS can be calculated by first-principles calculations, and lots of these materials show stronger piezoelectric coupling than traditional bulk wurtzite structures [5, 14–16]. As a result, these theories may enable one to gain a better understanding of some unique piezoelectric characteristics observed in experiments and atomic simulations. Spontaneously, piezotronic and piezo-phototronic effect of 2D materials have been developed for applications to electronics and optoelectronics, such as NGs for harvesting micromechniacal energy, photodetectors for optical sensors [9, 19].

Nowadays, experimental researches in piezotronic and piezo-phototronic effect of 2D materials have drawn a growing number of attention. The number of layers, piezoelectricity coefficient, and deformation directionality of the piezoelectric properties in MoS_2 have been studied systematically [9, 17]. Specifically, thin MoS_2 membrane with an even and odd number of layers generates a zero and finite piezoelectric response, respectively. A piezoelectric coefficient of $e_{11} = 2.9 \times 10^{-10}$ C m^{-1} was measured in free-standing monolayer MoS_2 [17]. At the same time, the NG with the armchair direction of MoS_2 is approximately two times higher than that with the zigzag direction of MoS_2 under the same strain [18]. Considering the shortcoming of monolayer TMDCs materials with insufficient mechanical durability, bilayers WSe_2 fabricated via turbostratic stacking with reliable piezoelectric properties has been reported [55]. Additionally, strain-gated flexible optoelectronics based on monolayer piezoelectric-semiconductor MoS_2 or p-n junction interface to tune the separation/transport of photogenerated carriers have been explored, and the piezo-phototronic effect can be utilized in implementing two-terminal atomic-layer-thick phototransistor [19, 62]. Finally, it can be predicted that piezotronic and piezo-phototronic effect of an increasing number of novel 2D materials may be observed in experimental study such as modified graphene, g-C_3N_4, BP, 2D perovskites.

2D materials offer a new choice for achieving desired construction of heterostructures, which not only comprise a large family of these materials vertical stack covering a rather broad range of properties [99–102], but also assemble 1D–2D or 3D–2D heterojunctions by harnessing the merits of both materials such as MoS_2-carbon nanotubes and MoS_2–GaN films [103–106]. A plethora of opportunities will appear when we apply piezotronic and piezo-phototronic effect in the heterostrctures to creat modern electronics and optoelectronics. Moreover, electrically driven modulating of the dielectric constant in MoS_2 layers has been expolred [107], which unlocks a new application field of MoS_2 nanomaterials for the construction of photonic circuits. It becomes possible that the refractive index of 2D materials can be modulated by piezotronic and piezo-phototronic effect. The phenomene may further tune laser when the 2D materials act as gain medium. However, it cannot be neglected that the existence of interface state make it tough to prepare the heterojunction devices. How to increase the stability of devices and reduce the expensive expense in material synthesis and preparation technology are another vital challenges. In a word, the research of piezotronic and piezo-phototronic effect in 2D materials represents another significant milestone towards embedding such infusive low-dimensional materials into future technologies such as high-performance integrated optoelectronic devices and systems, which also needs endeavors in the field of piezotronic and piezo-phototronic effect in 2D materials to satisfy a demand for future application such as high-performance human-electronics interfacing display, energy harvesting, smulti-functional systems and so on.

Acknowledgment

The authors thank the support from National Natural Science Foundation of China (No. 61405040, 51622205, 61675027, 51432005, 61505010 and 51502018), the support of national key R & D project from Minister of Science and Technology, China (2016YFA0202703), Beijing City Committee of science and technology (Z171100002017019) and the 'Thousand Talents' program of China for pioneering researchers and innovative teams.

ORCID iDs

Caofeng Pan https://orcid.org/0000-0001-6327-9692

References

[1] Zhang H 2015 Ultrathin two-dimensional nanomaterials *ACS Nano* **9** 9451
[2] Tan C *et al* 2017 Recent advances in ultrathin two-dimensional nanomaterials *Chem. Rev.* **117** 6225
[3] Novoselov K S, Geim A K, Morozov S V, Jiang D, Zhang Y, Dubonos S V, Grigorieva I V and Firsov A A 2004 Electric field effect in atomically thin carbon films *Science* **306** 666
[4] Manish Chhowalla H S S, Eda G, Li L-J, Loh L P and Zhang H 2013 The chemistry of two-dimensional layered transition metal dichalcogenide nanosheets *Nat. Chem.* **5** 263
[5] Michel K H and Verberck B 2009 Theory of elastic and piezoelectric effects in two-dimensional hexagonal boron nitride *Phys. Rev.* B **80** 224301
[6] Novoselov K S, Mishchenko A, Carvalho A and Castro Neto A H 2016 2D materials and van der Waals heterostructures *Science* **353** aac9439
[7] Cheng R, Jiang S, Chen Y, Liu Y, Weiss N, Cheng H C, Wu H, Huang Y and Duan X 2014 Few-layer molybdenum disulfide transistors and circuits for high-speed flexible electronics *Nat. Commun.* **5** 5143
[8] Withers F *et al* 2015 Light-emitting diodes by band-structure engineering in van der Waals heterostructures *Nat. Mater.* **14** 301
[9] Wu W *et al* 2014 Piezoelectricity of single-atomic-layer MoS_2 for energy conversion and piezotronics *Nature* **514** 470
[10] Fiori G, Bonaccorso F, Iannaccone G, Palacios T, Neumaier D, Seabaugh A, Banerjee S K and Colombo L 2014 Electronics based on two-dimensional materials *Nat. Nanotechnol.* **9** 768
[11] Xia F, Wang H, Xiao D, Dubey M and Ramasubramaniam A 2014 Two-dimensional material nanophotonics *Nat. Photon.* **8** 899
[12] Yang F, Cheng S, Zhang X, Ren X, Li R, Dong H and Hu W 2017 2D Organic Materials for optoelectronic applications *Adv. Mater.* **30** 1702415
[13] Michel K H and Verberck B 2011 Phonon dispersions and piezoelectricity in bulk and multilayers of hexagonal boron nitride *Phys. Rev.* B **83** 2720

[14] Duerloo K-a N, Ong M T and Reed E J 2012 Intrinsic piezoelectricity in two-dimensional materials *J. Phys. Chem. Lett.* **3** 2871

[15] Fei R, Li W, Li J and Yang L 2015 Giant piezoelectricity of monolayer group IV monochalcogenides: SnSe, SnS, GeSe, and GeS *Appl. Phys. Lett.* **107** 173104

[16] Li W and Li J 2015 Piezoelectricity in two-dimensional group-III monochalcogenides *Nano Res.* **8** 3796

[17] Zhu H, Wang Y, Xiao J, Liu M, Xiong S, Wong Z J, Ye Z, Ye Y, Yin X and Zhang X 2015 Observation of piezoelectricity in free-standing monolayer MoS_2 *Nat. Nanotechnol.* **10** 151

[18] Kim S K, Bhatia R, Kim T-H, Seol D, Kim J H, Kim H, Seung W, Kim Y, Lee Y H and Kim S-W 2016 Directional dependent piezoelectric effect in CVD grown monolayer MoS_2 for flexible piezoelectric nanogenerators *Nano Energy* **22** 483

[19] Wu W, Wang L, Yu R, Liu Y, Wei S H, Hone J and Wang Z L 2016 Piezophototronic effect in single-atomic-layer MoS_2 for strain-gated flexible optoelectronics *Adv. Mater.* **28** 8463

[20] Wu W and Wang Z L 2016 Piezotronics and piezo-phototronics for adaptive electronics and optoelectronics *Nat. Rev. Mater.* **1** 16031

[21] Wang Z L 2010 Piezopotential gated nanowire devices: Piezotronics and piezo-phototronics *Nano Today* **5** 540

[22] Wang Z L 2012 Preface to the special section on piezotronics *Adv. Mater.* **24** 4630

[23] He J H, Hsin C L, Liu J, Chen L J and Wang Z L 2007 Piezoelectric gated diode of a single ZnO nanowire *Adv. Mater.* **19** 781

[24] Yang Q, Guo X, Wang W, Zhang Y, Xu S, Lien D H and Wang Z L 2010 Enhancing sensitivity of a single ZnO micro-/nanowire photodetector by piezo-phototronic effect *ACS Nano* **4** 6285

[25] Wang Z L 2007 The new field of nanopiezotronics *Mater. Today* **10** 20

[26] Yang Q, Wang W, Xu S and Wang Z L 2011 Enhancing light emission of ZnO microwire-based diodes by piezo-phototronic effect *Nano Lett.* **11** 4012

[27] Zhonglin W 2012 *Piezotronics and Piezo-Phototronics* (Berlin: Springer)

[28] Zhang Y, Liu Y and Wang Z L 2011 Fundamental theory of piezotronics *Adv. Mater.* **23** 3004

[29] Pan C, Chen M, Yu R, Yang Q, Hu Y, Zhang Y and Wang Z L 2016 Progress in piezo-phototronic-effect-enhanced light-emitting diodes and pressure imaging *Adv. Mater.* **28** 1535

[30] Blonsky M N, Zhuang H L, Singh A K and Hennig R G 2015 *Ab initio* prediction of piezoelectricity in two-dimensional materials *ACS Nano* **9** 9885

[31] Reed E J 2015 Piezoelectricity: now in two dimensions *Nat. Nanotechnol.* **10** 106

[32] Radisavljevic B, Radenovic A, Brivio J, Giacometti V and Kis A 2011 Single-layer MoS_2 transistors *Nat. Nanotechnol.* **6** 147

[33] Wang Z L 2012 Progress in piezotronics and piezo-phototronics *Adv. Mater.* **24** 4632

[34] Ahmadpoor F and Sharma P 2015 Flexoelectricity in two-dimensional crystalline and biological membranes *Nanoscale* **7** 16555

[35] Mak K F, Lee C, Hone J, Shan J and Heinz T F 2010 Atomically thin MoS_2: a new direct-gap semiconductor *Phys. Rev. Lett.* **105** 136805

[36] Bertolazzi S, Brivio J and Kis A 2011 Stretching and breaking of ultrathin MoS_2 *ACS Nano* **5** 9703

[37] Castellanos-Gomez A, Poot M, Steele G A, Van Der Zant H S J, Agraït N and Rubio-Bollinger G 2012 Elastic properties of freely suspended MoS_2 nanosheets *Adv. Mater.* **24** 772

[38] Zhou Y, Liu W, Huang X, Zhang A, Zhang Y and Wang Z L 2016 Theoretical study on two-dimensional MoS_2 piezoelectric nanogenerators *Nano Res.* **9** 800

[39] Zheng D Q, Zhao Z, Huang R, Nie J, Li L and Zhang Y 2017 High-performance piezo-phototronic solar cell based on two-dimensional materials *Nano Energy* **32** 448

[40] Wang Z L and Song J 2006 Piezoelectric Nanogenerators based on zinc oxide nanowire arrays *Science* **312** 242

[41] Hu Y, Zhang Y, Chang Y, Snyder R L and Wang Z L 2010 Optimizing the power output of a ZnO photocell by piezopotential *ACS Nano* **4** 4220

[42] Pan C, Dong L, Zhu G, Niu S, Yu R, Yang Q, Liu Y and Wang Z L 2013 High-resolution electroluminescent imaging of pressure distribution using a piezoelectric nanowire LED array *Nat. Photon.* **7** 752

[43] Han X, Du W, Yu R, Pan C and Wang Z L 2015 Piezo-phototronic enhanced UV sensing based on a nanowire photodetector array *Adv. Mater.* **27** 7963

[44] Minary-Jolandan M, Bernal R A, Kuljanishvili I, Parpoil V and Espinosa H D 2012 Individual GaN nanowires exhibit strong piezoelectricity in 3D *Nano Lett.* **12** 970

[45] Lee C, Wei X, Kysar J W and Hone J 2008 Measurement of the elastic properties and intrinsic strength of monolayer graphene *Science* **321** 385

[46] Sevik C, akır D, Gülseren O and Peeters F M 2016 Peculiar piezoelectric properties of soft two-dimensional materials *J. Phys. Chem.* C **120** 13948

[47] Li Y, Rao Y, Mak K F, You Y, Wang S, Dean C R and Heinz T F 2013 Probing symmetry properties of few-layer MoS_2 and h-BN by optical second-harmonic generation *Nano Lett.* **13** 3329

[48] Qi J, Lan Y-W, Stieg A Z, Chen J-H, Zhong Y-L, Li L-J, Chen C-D, Zhang Y and Wang K L 2015 Piezoelectric effect in chemical vapour deposition-grown atomic-monolayer triangular molybdenum disulfide piezotronics *Nat. Commun.* **6** 7430

[49] Yu X, Han X, Zhao Z, Zhang J, Guo W, Pan C, Li A, Liu H and Lin Wang Z 2015 Hierarchical TiO_2 nanowire/graphite fiber photoelectrocatalysis setup powered by a wind-driven nanogenerator: A highly efficient photoelectrocatalytic device entirely based on renewable energy *Nano Energy* **11** 19

[50] Wang C, Bao R, Zhao K, Zhang T, Dong L and Pan C 2015 Enhanced emission intensity of vertical aligned flexible ZnO nanowire/p-polymer hybridized LED array by piezo-phototronic effect *Nano Energy* **14** 364

[51] Yang R, Qin Y, Dai L and Wang Z L 2008 Power generation with laterally packaged piezoelectric fine wires *Nat. Nanotechnol.* **4** 34

[52] He K, Poole C, Mak K F and Shan J 2013 Experimental demonstration of continuous electronic structure tuning via strain in atomically thin MoS_2 *Nano Lett.* **13** 2931

[53] Dean C R *et al* 2010 Boron nitride substrates for high-quality graphene electronics *Nat. Nanotechnol.* **5** 722

[54] Wang Z L and Wu W 2012 Nanotechnology-enabled energy harvesting for self-powered micro-/nanosystems *Angew. Chem., Int. Ed.* **51** 11700

[55] Lee J H *et al* 2017 Reliable piezoelectricity in bilayer WSe_2 for piezoelectric nanogenerators *Adv. Mater.* **29** 1606667

[56] Liu K *et al* 2014 Elastic properties of chemical-vapor-deposited monolayer MoS_2, WS_2, and their bilayer heterostructures *Nano Lett.* **14** 5097

[57] Hsu W-T, Zhao Z-A, Li L-J, Chen C-H, Chiu M-H, Chang P-S, Chou Y-C and Chang W-H 2014 Second harmonic generation from artificially stacked transition metal dichalcogenide twisted bilayers *ACS Nano* **8** 2951

[58] Puretzky A A, Liang L, Li X, Xiao K, Sumpter B G, Meunier V and Geohegan D B 2016 Twisted $MoSe_2$ bilayers with variable local stacking and interlayer coupling revealed by low-frequency raman spectroscopy *ACS Nano* **10** 2736

[59] Guo J, Wen R, Liu Y, Zhang K, Kou J, Zhai J and Wang Z L 2018 Piezotronic effect enhanced flexible humidity sensing of monolayer MoS_2 *ACS App.l Mater. Interfaces* **10** 8110

[60] Zhao J, Li N, Yu H, Wei Z, Liao M, Chen P, Wang S, Shi D, Sun Q and Zhang G 2017 Highly sensitive MoS_2 humidity sensors array for noncontact sensation *Adv. Mater.* **29** 1702076

[61] Zhang D, Wu J, Li P and Cao Y 2017 Room-temperature SO_2 gas-sensing properties based on a metal-doped MoS_2 nanoflower: an experimental and density functional theory investigation *J. Mater. Chem.* A **5** 20666

[62] Zhang K *et al* 2017 A flexible p-CuO/n-MoS_2 heterojunction photodetector with enhanced photoresponse by the piezo-phototronic effect *Mater. Horiz.* **4** 274

[63] Ke Z, Junyi Z and Zhong Lin Lin W 2018 A monolayer MoS_2 p-n homogenous photodiode with enhanced photoresponse by piezo-phototronic effect *2D Mater.* **5** 035038

[64] Kim D-H, Ghaffari R, Lu N and Rogers J A 2012 Flexible and stretchable electronics for biointegrated devices *Annu. Rev. Biomed. Eng.* **14** 113
[65] Morin S A, Shepherd R F, Kwok S W, Stokes A A, Nemiroski A and Whitesides G M 2012 Camouflage and display for soft machines *Science* **337** 828
[66] Zhao X, Hua Q, Yu R, Zhang Y and Pan C 2015 Flexible, stretchable and wearable multifunctional sensor array as artificial electronic skin for static and dynamic strain mapping *Adv. Electron. Mater.* **1** 1500142
[67] Choi M S, Qu D, Lee D, Liu X, Watanabe K, Taniguchi T and Yoo W J 2014 Lateral MoS_2 p–n junction formed by chemical doping for use in high-performance optoelectronics *ACS Nano* **8** 9332
[68] Li H-M, Lee D, Qu D, Liu X, Ryu J, Seabaugh A and Yoo W J 2015 Ultimate thin vertical p–n junction composed of two-dimensional layered molybdenum disulfide *Nat. Commun.* **6** 6564
[69] Zhao Y, Xu K, Pan F, Zhou C, Zhou F and Chai Y 2016 Doping, contact and interface engineering of two-dimensional layered transition metal dichalcogenides transistors *Adv. Func. Mater.* **27** 1603484
[70] Zhang J and Meguid S A 2017 Piezoelectricity of 2D nanomaterials: characterization, properties, and applications *Semicond. Sci. Technol.* **32** 043006
[71] Akinwande D, Petrone N and Hone J 2014 Two-dimensional flexible nanoelectronics *Nat. Commun.* **5** 5678
[72] Ruh D, Reith P, Sherman S, Theodor M, Ruhhammer J, Seifert A and Zappe H 2014 Stretchable optoelectronic circuits embedded in a polymer network *Adv. Mater.* **26** 1706
[73] Zhang Y, Tang T-T, Girit C, Hao Z, Martin M C, Zettl A, Crommie M F, Shen Y R and Wang F 2009 Direct observation of a widely tunable bandgap in bilayer graphene *Nature* **459** 820
[74] Zhou S Y, Gweon G H, Fedorov A V, First P N, De Heer W A, Lee D H, Guinea F, Castro Neto A H and Lanzara A 2007 Substrate-induced bandgap opening in epitaxial graphene *Nat. Mater.* **6** 770
[75] Balog R *et al* 2010 Bandgap opening in graphene induced by patterned hydrogen adsorption *Nat. Mater.* **9** 315
[76] Ong M T and Reed E J 2012 Engineered piezoelectricity in graphene *ACS Nano* **6** 1387
[77] Chandratre S and Sharma P 2012 Coaxing graphene to be piezoelectric *Appl. Phys. Lett.* **100** 023114
[78] Zelisko M, Hanlumyuang Y, Yang S, Liu Y, Lei C, Li J, Ajayan P M and Sharma P 2014 Anomalous piezoelectricity in two-dimensional graphene nitride nanosheets *Nat. Commun.* **5** 4284
[79] Ding R, Zhang X and Sun X W 2017 Organometal trihalide perovskites with intriguing ferroelectric and piezoelectric properties *Adv. Funct. Mater.* **27** 1702207
[80] Dou L *et al* 2015 Atomically thin two-dimensional organic-inorganic hybrid perovskites *Science* **349** 1518
[81] Tao J *et al* 2015 Mechanical and electrical anisotropy of few-layer black phosphorus *ACS Nano* **9** 11362
[82] El-Kelany K E, Carbonnière P, Erba A and Rérat M 2015 Inducing a finite in-plane piezoelectricity in graphene with low concentration of inversion symmetry-breaking defects *J. Phys. Chem.* C **119** 8966
[83] Da Cunha Rodrigues G, Zelenovskiy P, Romanyuk K, Luchkin S, Kopelevich Y and Kholkin A 2015 Strong piezoelectricity in single-layer graphene deposited on SiO_2 grating substrates *Nat. Commun.* **6** 7572
[84] De La Pierre M, Karamanis P, Baima J, Orlando R, Pouchan C and Dovesi R 2013 *Ab initio* periodic simulation of the spectroscopic and optical properties of novel porous graphene phases *J. Phys. Chem.* C **117** 2222
[85] Naumov I I and Bratkovsky A M 2011 Gap opening in graphene by simple periodic inhomogeneous strain *Phys. Rev.* B **84** 245444
[86] Shi Y, Kim K K, Reina A, Hofmann M, Li L-J and Kong J 2010 Work function engineering of graphene electrode via chemical doping *ACS Nano* **4** 2689
[87] Usachov D *et al* 2011 Nitrogen-doped graphene: efficient growth, structure, and electronic properties *Nano Lett.* **11** 5401
[88] Ci L *et al* 2010 Atomic layers of hybridized boron nitride and graphene domains *Nat. Mater.* **9** 430
[89] Shemella P and Nayak S K 2009 Electronic structure and band-gap modulation of graphene via substrate surface chemistry *Appl. Phys. Lett.* **94** 032101
[90] Bieri M *et al* 2009 Porous graphenes: two-dimensional polymer synthesis with atomic precision *Chem. Commun.* **45** 6919
[91] Zheng Y, Liu J, Liang J, Jaroniec M and Qiao S Z 2012 Graphitic carbon nitride materials: controllable synthesis and applications in fuel cells and photocatalysis *Energy Environ. Sci.* **5** 6717
[92] Li L, Yu Y, Ye G J, Ge Q, Ou X, Wu H, Feng D, Chen X H and Zhang Y 2014 Black phosphorus field-effect transistors *Nat. Nanotechnol.* **9** 372
[93] Huang L, Li Y, Wei Z and Li J 2015 Strain induced piezoelectric effect in black phosphorus and MoS_2 van der Waals heterostructure *Sci. Rep.* **5** 16448
[94] Goodman G 1963 Electrical conduction anomaly in samarium-doped barium titanate *J. Am. Ceram. Soc.* **46** 48
[95] Qian X, Wang Y, Li W, Lu J and Li J 2015 Modelling of stacked 2D materials and devices *2D Mater.* **2** 032003
[96] Wang F, Wang Z, Jiang C, Yin L, Cheng R, Zhan X, Xu K, Wang F, Zhang Y and He J 2017 Progress on electronic and optoelectronic devices of 2D layered semiconducting materials *Small* **13** 1604298
[97] Alidoust N *et al* 2014 Observation of monolayer valence band spin-orbit effect and induced quantum well states in MoX_2 *Nat. Commun.* **5** 4673
[98] Youngblood N, Chen C, Koester S J and Li M 2015 Waveguide-integrated black phosphorus photodetector with high responsivity and low dark current *Nat. Photon.* **9** 247
[99] Li M-Y *et al* 2015 Epitaxial growth of a monolayer WSe_2-MoS_2 lateral p-n junction with an atomically sharp interface *Science* **349** 524
[100] Chiu M-H, Zhang C, Shiu H-W, Chuu C-P, Chen C-H, Chang C-Y S, Chen C-H, Chou M-Y, Shih C-K and Li L-J 2015 Determination of band alignment in the single-layer MoS_2/WSe_2 heterojunction *Nat. Commun.* **6** 7666
[101] Huo N, Kang J, Wei Z, Li S-S, Li J and Wei S-H 2014 Novel and enhanced optoelectronic performances of multilayer MoS_2–WS_2 heterostructure transistors *Adv. Funct. Mater.* **24** 7025
[102] Hong X, Kim J, Shi S-F, Zhang Y, Jin C, Sun Y, Tongay S, Wu J, Zhang Y and Wang F 2014 Ultrafast charge transfer in atomically thin MoS_2/WS_2 heterostructures *Nat. Nanotechnol.* **9** 682
[103] Jariwala D, Sangwan V K, Wu C-C, Prabhumirashi P L, Geier M L, Marks T J, Lauhon L J and Hersam M C 2013 Gate-tunable carbon nanotube–MoS_2 heterojunction p-n diode *Proc. Natl Acad. Sci.* **110** 18076
[104] Xue F, Yang L, Chen M, Chen J, Yang X, Wang L, Chen L, Pan C and Wang Z L 2017 Enhanced photoresponsivity of the MoS_2-GaN heterojunction diode via the piezo-phototronic effect *NPG Asia Mater.* **9** e418
[105] Xue F *et al* 2016 P-type MoS_2 and n-type ZnO diode and its performance enhancement by the piezophototronic effect *Adv. Mater.* **28** 3391
[106] Liu X *et al* 2016 Enhancing photoresponsivity of self-aligned MoS_2 field-effect transistors by piezo-phototronic effect from GaN nanowires *ACS Nano* **10** 7451
[107] Santos E J G and Kaxiras E 2013 Electrically driven tuning of the dielectric constant in MoS_2 layers *ACS Nano* **7** 10741